arXiv:1404.1779v1 [physics.plasm-ph] 7 Apr 2014

Near infrared few-cycle pulses for high harmonic generation

Steffen Driever[a], Konstantin B. Holzner[a], Jean-Christophe Delagnes[b], Nikita Fedorov[b], Martin Arnold[a], Damien Bigourd[a], Eric Cormier[b], Roland Guichard[a], Eric Constant[b] and Amelle Zaïr[a]

[a]Imperial College London, Department of Physics, Blackett Laboratory Laser Consortium, London SW7 2AZ United Kingdom
[b]Université de Bordeaux, CEA, CNRS UMR 5107, CELIA (Centre Lasers Intenses et Applications), FR-33400 Talence, France

E-mail: steffen.driever10@imperial.ac.uk

Abstract. We report on the development of tunable few-cycle pulses with central wavelengths from 1.6 μm to 2 μm. Theses pulses were used as a proof of principle for high harmonic generation in atomic and molecular targets. In order to generate such pulses we produced a filament in a 4 bar krypton cell. Spectral broadening by a factor of 2 - 3 of a 40 fs near infrared input pulse was achieved. The spectrally broadened output pulses were then compressed by fused silica plates down to the few-cycle regime close to the Fourier limit. The auto-correlation of these pulses revealed durations of ~ 3 cycles for all investigated central wavelengths. Pulses with a central wavelength of 1.7 μm and up to 430 μJ energy per pulse were employed to generate high order harmonics in Xe, Ar and N_2. Moving to near infrared few-cycle pulses opens the possibility to operate deeply in the non-perturbative regime with a Keldysh parameter $\gamma << 1$. Hence, this source is suitable for the study of the non-adiabatic tunneling regime in most generating systems used for high order harmonic generation and attoscience.

1. Introduction:

During the interaction of intense laser fields with atoms and molecules an electron wavepacket initially bound to the target can be ionized through different interaction processes. These ionization channels determine the evolution of the core and the electron wavepacket in the continuum. To identify which of these processes is predominant during the interaction, L. V. Keldysh [1] introduced a parameter given by $\gamma = \sqrt{I_p/2U_p}$ where I_p is the target's ionization potential and U_p is the ponderomotive energy associated with the strong laser field employed.

In the perturbative regime, $\gamma >> 1$, the target's potential remains largely unchanged by the laser field. In this case multi-photon processes are necessary to emit a single electron wavepacket from the ground state. The electron wavepacket can absorb many photons, reaching energies just exceeding the ionization potential (MPI: multi-photon ionization), or absorb many more photons to overcome the ionization potential. After ionization, the electron wavepacket in the continuum can be considered only subject to the laser field [2, 3, 4]. When the laser field reverses half a cycle later the electron wavepacket can be redirected to the ionic core and then re-scatter (ATI: Above Threshold Ionization [5]).

When $\gamma << 1$, known as the non-perturbative regime, the target's potential is deformed by the strong laser field. This deformation happens at every maximum of the laser field, i.e. twice per optical cycle. Every optical half-cycle, the electron wavepacket initially bound to the target, sees the tail of the Coulomb potential evolve in time, hence creating a barrier whose height and width change over time. Thus, the electron wavepacket reaches a greater probability to tunnel out of the system through this potential barrier. The probability of tunneling through the barrier increases with the laser field strength to the point where the barrier drops below the binding energy level and the electron wavepacket is directly launched into the continuum (BSI: Barrier Suppression Ionization). The latter situation is the asymptotic limit of the tunnel ionization regime and usually results in an electron wavepacket which cannot be redirected by the laser field back to the ionic core. As a result recombination or re-scattering of the electron wavepacket does not occur.

In order to understand how ionization occurs we need to follow the transition between the different regimes of ionization. To study these transitions, most of the experiments were performed using an IR laser field ($0.8\,\mu m$) with a typical intensity of $I = 10^{14}\,W/cm^2$, interacting with atoms (noble gases) [3, 4, 6, 7], molecules [8], nanoparticles [9, 10, 11] or periodic solid structures [12, 13]. For these targets, the ionization potential is kept below $\sim 25\,\mathrm{eV}$, so that ionization regimes correspond to γ values between 0.5 and ~ 5. Under such conditions, only high I_p atoms subject to a strong laser field are in the non-perturbative regime. To enable the study of dynamical processes under the non-perturbative regime for most atoms and molecules two routes can be followed.

Firstly, one can increase the laser field intensity keeping the wavelength in the infrared (IR) region ($0.8\,\mu m$ for instance). This approach has been employed widely owing to the development of Ti:Sa laser technologies [14]. However it is strongly limited by the field strength that a target can withstand before its ground state is strongly depleted. One way to circumvent this limitation is to use few-cycle pulses and to control their intensity profile. In this case one has to reconsider the Keldysh parameter in a non-quasi static situation as shown by Yudin and Ivanov [15]. They defined a general expression for non-adiabatic ionization rates based on a modification of the ADK theory [16] suitable for the case of few-cycle laser fields.

The second route is to decrease γ by increasing wavelengths (λ) to the near (NIR)or mid-infrared (MIR) region whilst maintaining low enough intensity to avoid depletion of the ground state. As a result it is possible to study the ultrafast dynamics of charge migration involved in atoms and molecules after ionization using high harmonic generation (HHG) [17, 18, 19, 20, 21, 22, 23, 24, 25]. However, analyzing HHG driven by few-cycle NIR to MIR pulses offers the possibility to extend these studies well into the non-perturbative regime and study how these charge migrations evolve while transitioning from one regime of ionization to another.

2. Employing a NIR to MIR laser field for high order harmonic generation

In recent years, efforts have been made to push the development of multi-cycle NIR to MIR femtosecond sources to drive strong field interaction such as HHG experiments. Indeed, using laser fields at longer wavelengths, i.e. in the low frequency limit to generate high order harmonics has the potential to dramatically extend the maximum photon energy produced (cut-off position). This is because it scales with $\propto \lambda^2$ [2, 3, 26, 27] and goes beyond the carbon K-edge. Hence, the coherent XUV and X-ray radiation produced can provide a unique source to study ultrafast inner core dynamics [28] opening the possibility to produce isolated attosecond pulses in the soft X-ray regime [29, 30]. However, the efficiency of the high harmonic generation process decreases when employing laser fields at longer wavelength as it drops with $\lambda^{-5.5}$ [31, 32, 33] which can limit the detection. Nevertheless experimentally, Colosimo *et al.* have succeeded in studying the wavelength scaling of the harmonic generation employing multi-cycle laser fields at $0.8\,\mu m$, $1.3\,\mu m$, $2\,\mu m$ and $3.6\,\mu m$ [34]. In their case the Keldysh parameter was varied from 1.3 to 0.3. Henceforth, they could resolve the transition from multi-photon behavior to the classical limit at the longest wavelength. Besides experimental work, the theory was adapted to the wavelength region up to $5\,\mu m$ to match the experimental data for high harmonic generation [32].

To access more complex dynamics under the non-perturbative regime Ghimire *et al.* [35] demonstrated the generation of high harmonics in periodic solid structures using multi-cycle MIR laser sources. This experiment enabled access to intraband currents

of these structures on the attosecond timescale. Transitions between bands of states within solids have already been described by Keldysh [1]. Thus, the transition rate of structure bands appears to be similar to that of the tunneling rate in atoms. This study has been extended further to cosine band structures for time-averaged transition rates [36].

Hawkins and Ivanov [37] have derived an analytic approximation for the transition rate in the low frequency limit to describe intraband sub-cycle electron dynamics. They showed that the transition depends on the band structure. This is due to electron acceleration after and during transition to the conduction band. Therefore, to really access time-dependent sub-cycle electron dynamics in atoms, molecules or periodic structures, it is crucial to employ few-cycle NIR or MIR sources. In this article we show the possibility to produce tunable few-cycle pulses via filamentation with central wavelengths tuned from 1.6 to $2\,\mu m$. As a proof of principle we show how this source can be used to drive HHG experiments in atoms and molecules. This opens the potential to investigate sub-cycle dynamics of various targets in the non-perturbative regime.

3. Adiabatic versus non-adiabatic Keldysh parameter in the low frequency limit

When $\gamma \ll 1$ which is the case for long wavelengths (low-frequency limit) and high intensities, the ionization rate for hydrogen atoms described by Keldysh [1] coincides with the well known tunnel ionization formula for static fields [38, 39]. In particular, the exponential dependence of the rate with respect to the field amplitude is present. When $\gamma \gg 1$, the formula reduces to a sum describing the ionization via the simultaneous absorption of several photons. In the tunneling case, i.e. $\gamma \ll 1$, the adiabatic approximation holds and the atomic structure can be reintroduced by means of an effective n^*, and the usual ℓ and m quantum numbers in the exponential prefactor [40]. This approach has been further extended to any arbitrary ionic state by Ammosov *et al.* [16] which is today known as the ADK theory.

The results of these formulae are in excellent agreement with experimental measurements [41] accounting for cycle-average rates over one half-period of the alternating electric field, under the assumption of a sufficiently slow varying envelope between two consecutives cycles. With the possibility to produce and design few-cycle laser pulses, which is the frame of this article, this assumption is not valid anymore. Therefore, one has to use the non-adiabatic ionization rate formula developed by Yudin and Ivanov [15] for any arbitrary γ:

$$\Gamma(t) = N(t) \exp\left(-\frac{E_0^2 f(t)^2}{\omega^3} \Phi\left(\gamma(t), \theta(t)\right)\right). \tag{1}$$

It explicitly takes into account the sub-cycle dynamics through the envelope $f(t)$ expressed in the time dependent Keldysh parameter $\gamma(t) = \gamma/f(t)$ and in $N(t)$ and through the instantaneous laser phase $\theta(t) = \omega t + \phi_0$ [15]. We applied this formula to

the calculation of the ionization probability of argon by 3-cycle pulses generated at an intensity of 10^{14} W/cm^2 and for 1.7μm, 1.8μm and 1.9 μm wavelengths (cf. figure 1). Once again, these long wavelengths ensure to be in 'better' tunneling conditions than the usual experiments at 0.8 μm and the 3-cycle pulse justifies the use of eq. (1).

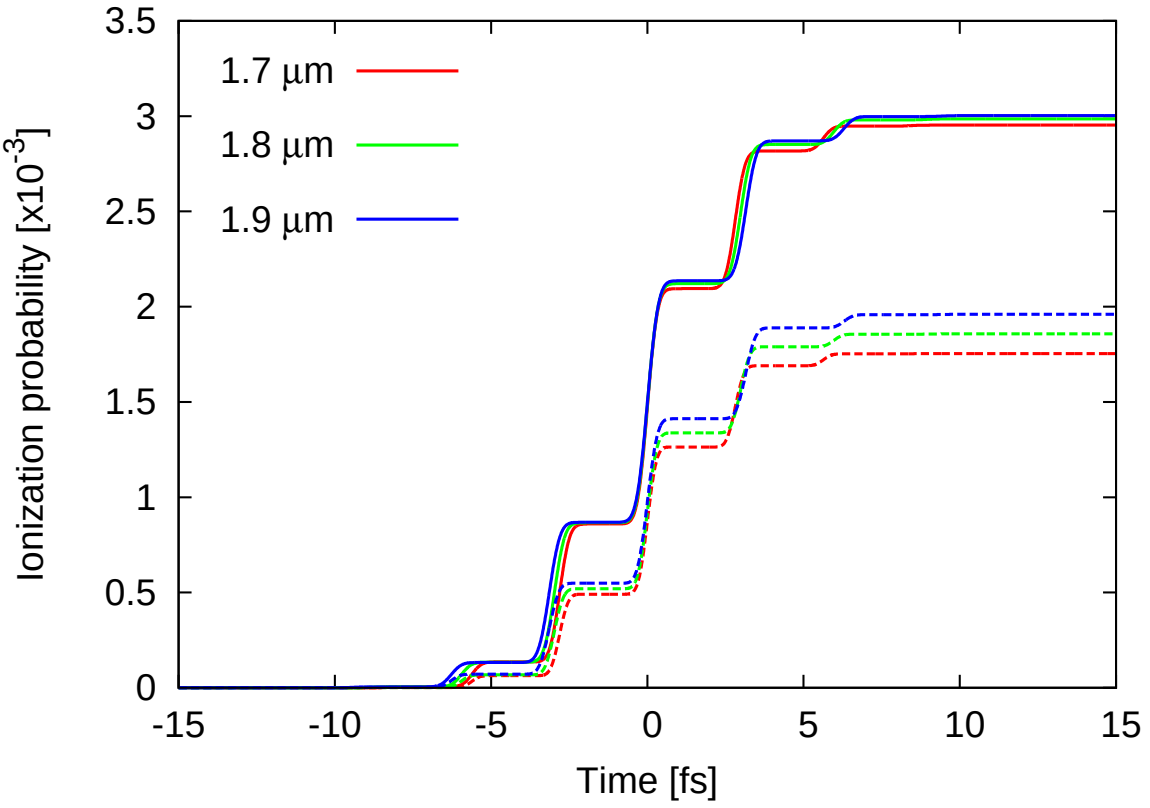

Figure 1. Non-adiabatic ionization probabilities calculated in argon for 3-cycle Gaussian pulses, $\lambda = 1.7\mu m$, 1.8μm and 1.9 μm, $I = 10^{14}$ W/cm^2 and $\phi_0 = 0$ (solid lines) compared to ADK ionization rates (dashed lines).

Clearly, non-adiabatic ionization probabilities (solid lines) build up in a stepwise manner during the laser interaction but do not differ much at the end of the pulse for all considered wavelengths. By comparison, ADK ionization probabilities are lower by a factor of 1.5 to 1.7 and the probabilities are separated further when the interaction is over. This shows the strong influence of the sub-cycle dynamics on the ionization processes and the necessity to take them into account when a theoretical description is required in such conditions, i.e. for HHG experiments. It is worth mentioning that these two calculations asymptotically converge for $\omega \to 0$.

4. Production of tunable NIR few-cycle pulses by filamentation

Few-cycle pulses have been generated via various methods in the IR over the last decade. The two most common methods are hollow core fiber compression [42] and filamentation [43, 44, 45, 46]. These are used in a post-compression scheme after the amplifier system.

These techniques have been successfully adapted to the spectral region beyond the Ti:Sa wavelength of $0.8\,\mu m$ and have been investigated experimentally as well as theoretically [44, 45, 47, 48]. In the $2\,\mu m$ regime an optical parametric amplifier (OPA) scheme was used by Hauri *et al.* generating 55 fs, $330\,\mu$J with carrier envelope stability [45]. By filamentation in a xenon cell they managed to compress the input pulse down to 17 fs with $270\,\mu$J pulse energy. Further, supercontinua spanning up to 3 octaves have been demonstrated by Kartoshov *et al.* stretching from $\sim 0.35\,\mu m$ - $5\,\mu m$ [49] employing a 80 fs, 20 Hz laser with a central wavelength of $3.9\,\mu m$. Mücke *et al.* [50] focused specifically on using $1.5\,\mu m$ and managed to achieve a compression factor of 3 - 4 with pulses as short as 19 fs and 1.5 mJ pulse energy generated in an argon cell.
In parallel to these studies, the very well established hollow core fiber compression technique has been used at $1.8\,\mu m$ to generate 11.5 fs pulses at $400\,\mu$J of pulse energy [51]. These studies show how post-compression can be employed to produce few-cycle pulses in the NIR to MIR region. The next step is to show if conditions can be found to provide tunability of these sources.
A first study was performed using filamentation to generate tunable few-cycle pulses in the region of $1\,\mu m$- $2\,\mu m$ [52] but it was not clearly shown if the pulse energy was sufficient to perform strong field interaction in the non-perturbative regime. We demonstrated the capability of filamentation to produce $1.6\,\mu m$- $2\,\mu m$ tunable few-cycle pulses [53] and we report in this article how these pulses provide sufficient energy per pulse to produce non-perturbative HHG in Xe, Ar and N_2 molecules.

5. Experiment

In order to generate the few-cycle pulses needed we employed an optical parametric amplifier (OPA) which generated $1.6\,\mu m$ - $2\,\mu m$ radiation with a pulse duration of 40 fs. It was seeded by $0.8\,\mu m$, 1 kHz, 40 fs, 5 mJ pulses from a Ti:Sa amplifier. The generated NIR beam is produced with $0.7\,\mu$J - $0.9\,\mu$J pulse energy and was loosely focused with a f=75 cm concave mirror. The 1.2 m cell was filled with 4 bar of krypton. The cell was sealed with 1 mm windows with an anti-reflection coating spanning $1.2\,\mu m$ - $2.2\mu m$.
In the generated filament, mainly self-phase modulation (SPM) contributes to the spectral broadening, but other effects like self-steepening can create a pedestal on the blue side. Further, ionization blue shift of the fundamental wavelength and high-order Kerr effects can also be involved. We showed in a recent study how tunable spectral broadening and compression from $1.6\,\mu m$ - $2\,\mu m$ can be produced [53]. Figure 2 shows an example of the tunable spectral broadening and compression obtained. We managed to generate 3-cycle pulses for several central wavelengths of the OPA. The spectrum was broadened in the filamentation process by a factor of 2 - 3 to 250 - 300 nm full width half maximum.
The accumulated positive group delay dispersion (GDD) was compensated by ~ 4 mm of fused silica. Since the fused silica has a negative GDD for these wavelengths it was robust and straight forward to compensate for the phase. For $1.7\,\mu m$ and $1.9\,\mu m$ we

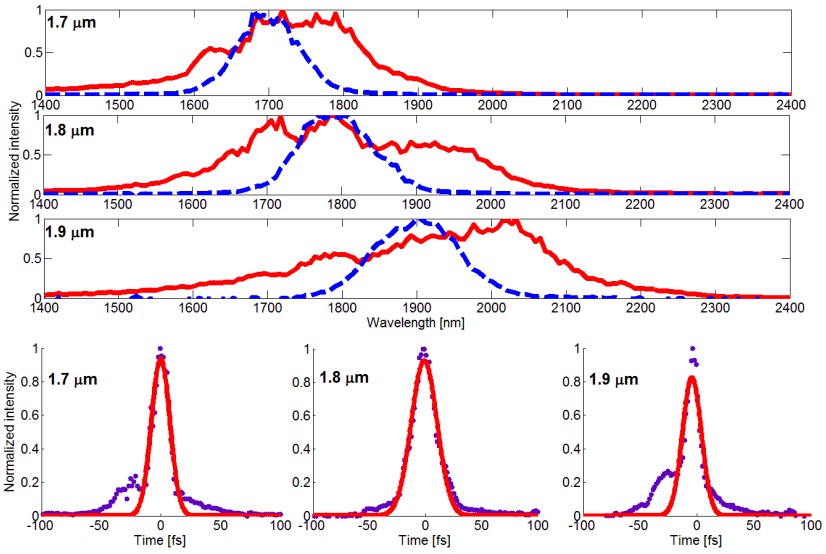

Figure 2. Upper panel: Input spectra (blue, dashed), spectra after filamentation (red, solid). Lower panel: auto-correlation for 1.7 μm, 1.8 μm and 1.9 μm. The purple dots are experimental data, the pulse width is given by the Gaussian fit. The fit gives 15 fs for 1.7μm and 1.9 μm whereas 1.8 μm reveals a pulse duration of 18 fs. The Fourier limit of 1.7μm and 1.9 μm was 12 fs and the Fourier limit of 1.8 μm was 15 fs.

generated pulses of $\sim$15 fs duration, whereas at 1.8 μm the duration was $\sim$18 fs. The auto-correlation was very close to the Fourier limit of 12 fs for 1.7 μm and 1.9 μm and 15 fs for 1.8 μm.

We employed the 1.7 μm filament for our high harmonic generation (HHG) experiment after identifying the filament size [54]. The centroid of the spectrum changed to 1.74 μm in the process. The size of the filament is defined as the region with the widest broadening and was estimated to $\sim$5 mm.Selecting this spatial region ensures that we only use the few-cycle pulses in our interaction region.

The high harmonics were generated subsequently in a semi-infinite cell (SIC) in vacuum, sealed with a 1 mm fused silica window and an output stainless steel foil (150 μm) at the exit. The 15 fs pulses centered at 1.74 μm were focused by a f=30 cm mirror (denoted FM) resulting in an interaction length of $\sim$30 mm (cell size). The SIC output foil was drilled by the laser itself providing an additional differential pumping stage. The pressure can subsequently be used as an additional degree of freedom to enable efficient HHG. The beam size at the entrance and exit of the cell was estimated to be 260 μm and 65 μm respectively. Due to the fact that we focused on the output foil of the SIC, short and long trajectories for HHG can be phase matched [55, 56]. This however is mitigated by the long interaction region which results in a harmonic spectrum solely due to the short trajectories. The generated HHG is subsequently redirected to a 600 lines/mm XUV grating (denoted G) at grazing incidence. The separated wavelengths are redirected with a toroidal mirror (denoted TM) onto the multi-channel plate (MCP) with phosphor screen and CCD camera. The experimental

setup is shown in figure 3.

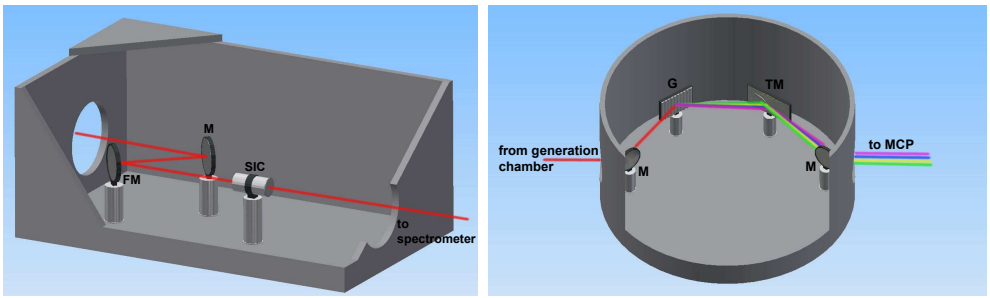

Figure 3. Schematic of the experimental setup. After entering the generation chamber (left), the beam is redirected (mirror M) and focused (focusing mirror FM) to the interaction region in the semi-infinite cell (SIC). The beam then enters the XUV spectrometer chamber (right). The grating (G) disperses the harmonics and the toroidal mirror (TM) images the spectra onto the MCP.

6. Results

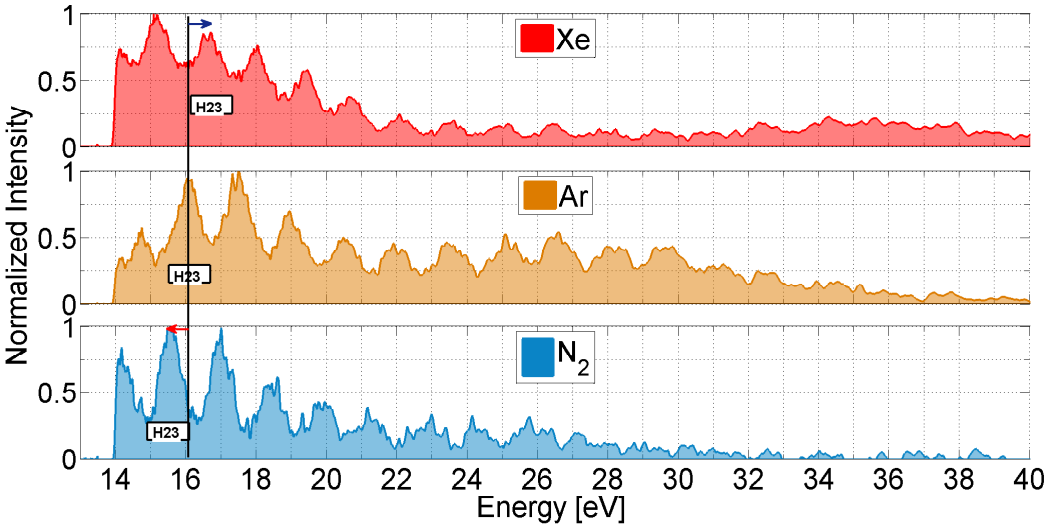

Figure 4. High harmonic spectra for xenon, argon and nitrogen for optimized generation conditions, top to bottom.

In figure 4 from top to bottom the HHG spectra for xenon, argon and nitrogen are presented. The current observation window reaches from 14 to 50 eV. The xenon spectrum was acquired for a pressure of 41 mbar and 180 μJ. This should lead to a cut-off energy of $E_{cut-off}$=(3.17U_p+1.3I_p) = 93.95 eV (I_p(Xe)=12.13 eV) at the focus which is at the end of the cell. Estimating the maximum photon energy from the intensity at the entrance of the cell we can expect a cut-off at 20.6 eV. The best spectrum for argon was obtained for 85 mbar and 430 μJ potentially generating harmonics up to 200.9 eV (I_p(Ar)=15.76 eV) at the focus. Considering the intensity at the entrance of the cell we

estimated a cut-off energy of 32 eV. The N_2 spectra on the other hand were generated at 105 mbar and 320 μJ pulse energy ($E_{max-cut-off}$= 154.8 eV, $I_p(N_2)$=15.58 eV). The minimum cut-off energy should be about 28.4 eV. The pressure ratio between xenon and argon $P_{argon}/P_{xenon} \sim 2.1$ (respectively nitrogen molecules and argon $P_{argon}/P_{N_2} \sim 0.81$) is close to the square root of the inverse ratio of their masses $\sqrt{M_{xenon}/M_{argon}} = 1.73$ (respectively $\sqrt{M_{N_2}/M_{argon}} = 0.87$), so that the density of emitters for HHG in the volume of interaction is comparable.
In xenon (lower I_p medium than argon) the high harmonic are blue shifted with respect to the argon high harmonics. As an example shown in figure 4, the 23^{rd} harmonic in xenon is blue shifted by half a photon energy at 1.74 μm with respect to the 23^{rd} in argon. This is due to the generation of plasma in xenon that modifies the fundamental pulse spectra towards lower wavelengths [57] as the saturation intensity of xenon ($8.2 \times 10^{13} W/cm^2$) is lower than in argon ($2.3 \times 10^{14} W/cm^2$) . The N_2 HHG spectrum on the contrary is not blue shifted with respect to the argon (both have similar I_p so similar saturation intensity) but it is red shifted. The 23^{rd} harmonic shown in figure 4 is red shifted by one photon energy at 1.74 μm due to the Raman effect [58]. The first Stokes shift due to a rotational effect from N_2 ($12\,cm^{-1}$) induces a fundamental central wavelength shift of 1.5 nm which is too small to compare to the spectral bandwidth of our few-cycle pulse. However over a long interaction region in the SIC, a cascade of first Stoke shift can occur resulting in a shift of multiple nm from the central wavelength (amplified Raman effect).

7. Conclusion and Outlook

We managed to produce tunable few-cycle pulses in the NIR using filamentation. These NIR few-cycle pulses have sufficient energy per pulse to enable the generation of high order harmonics in the non-perturbative regime. The results presented using these pulses for HHG are very promising as they reveal effects of free electrons and Raman cascading encoded in the HHG spectra. This tunable source will enable the study of transitions between ionization regimes of atomic and molecular targets in gas or condensate phase.

8. Acknowledgment

This work was supported by UK-EPSRC project EP/ J002348/1CADAM,UK Royal Society project IE120539, Laserlab-Europe III CNRSCELIA001889, Inrex laserlab-europe III JRA, the region aquitaine (Nasa project) and the ANR attowave project. The authors acknowledge technical support from D. Descamps and F. Burgy from CELIA and P. Ruthven and A. Gregory from Imperial College London.

References

[1] Keldysh L V 1964 Zh. Eksp. Teor. Fiz.47 1945
Keldysh L V 1965 Sov. Phys.JETP 20 1307 (Engl. transl.)

[2] Lewenstein, M., Balcou, P., Ivanov, M.Y., L'Huillier, A., Corkum, P.B., 1994. Theory of high-harmonic generation by low-frequency laser fields. Phys. Rev. A 49, 2117 —2132.

[3] Corkum, P.B., 1993. Plasma perspective on strong field multiphoton ionization. Phys. Rev. Lett. 71, 1994 —1997.

[4] Schafer, K.J., Yang, B., DiMauro, L.F., Kulander, K.C., 1993. Above threshold ionization beyond the high harmonic cutoff. Phys. Rev. Lett. 70, 1599—1602.

[5] Agostini, P., Fabre, F., Mainfray, G., Petite, G., Rahman, N., 1979. Free-Free Transitions Following Six-Photon Ionization of Xenon Atoms. Physical Review Letters 42, 1127 —1130.

[6] L'Huillier, A., Balcou, P., Candel, S., Schafer, K.J., Kulander, K.C., 1992. Calculations of high-order harmonic-generation processes in xenon at 1064 nm. Phys. Rev. A 46, 2778 —2790.

[7] L'Huillier, A., Balcou, P., 1993. High-order harmonic generation in rare gases with a 1-ps 1053-nm laser. Phys. Rev. Lett. 70, 774 —777.

[8] Fraser, D.J., Hutchinson, M.H.R., Marangos, J.P., Shao, Y.L., Tisch, J.W.G., Castillejo, M., 1995. High harmonic generation in butane and butadiene. J. Phys. B: At. Mol. Opt. Phys. 28, L739.

[9] Kim, S., Jin, J., Kim, Y.-J., Park, I.-Y., Kim, Y., Kim, S.-W., 2008. High-harmonic generation by resonant plasmon field enhancement. Nature 453, 757 —760.

[10] Shaaran, T., Ciappina, M.F., Guichard, R., Pérez-Hernández, J.A., Roso, L., Arnold, M., Siegel, T., Zaïr, A., Lewenstein, M., 2013. High-order-harmonic generation by enhanced plasmonic near-fields in metal nanoparticles. Phys. Rev. A 87, 041402.

[11] Süßmann, F., Kling, M.F., 2011. Attosecond nanoplasmonic streaking of localized fields near metal nanospheres. Phys. Rev. B 84, 121406.

[12] Schiffrin, A., Paasch-Colberg, T., Karpowicz, N., Apalkov, V., Gerster, D., Mühlbrandt, S., Korbman, M., Reichert, J., Schultze, M., Holzner, S., Barth, J.V., Kienberger, R., Ernstorfer, R., Yakovlev, V.S., Stockman, M.I., Krausz, F., 2013. Optical-field-induced current in dielectrics. Nature 493, 70 —74.

[13] Apalkov, V., Stockman, M.I., 2012. Theory of dielectric nanofilms in strong ultrafast optical fields. Phys. Rev. B 86, 165118.

[14] Moulton, P.F., 1986. Spectroscopic and laser characteristics of Ti:Al_2O_3. Journal of the Optical Society of America B 3, 125.

[15] Yudin, G.L., Ivanov, M.Y., 2001. Nonadiabatic tunnel ionization: Looking inside a laser cycle. Phys. Rev. A 64, 013409.

[16] Ammosov, M. V., Delone, N. B. and Krainov, V. P., 1986, Tunnel ionization of complex atoms and atomic ions by an alternating electromagnetic field, Sov. Phys. JETP 64, 1191 —1194

[17] Baker, S., Robinson, J.S., Haworth, C.A., Teng, H., Smith, R.A., Chirilă, C.C., Lein, M., Tisch, J.W.G., Marangos, J.P., 2006. Probing Proton Dynamics in Molecules on an Attosecond Time Scale. Science 312, 424 —427.

[18] Marangos, J.P., Baker, S., Kajumba, N., Robinson, J.S., Tisch, J.W.G., Torres, R., 2007. Dynamic imaging of molecules using high order harmonic generation. Phys. Chem. Chem. Phys. 10, 35 —48.

[19] Lein, M., 2007. Molecular imaging using recolliding electrons. Journal of Physics B: Atomic, Molecular and Optical Physics 40, R135R173.

[20] Itatani, J., Levesque, J., Zeidler, D., Niikura, H., Pépin, H., Kieffer, J.C., Corkum, P.B., Villeneuve, D.M., 2004. Tomographic imaging of molecular orbitals. Nature 432, 867 —871.

[21] Hässler, S., Caillat, J., Boutu, W., Giovanetti-Teixeira, C., Ruchon, T., Auguste, T., Diveki, Z., Breger, P., Maquet, A., Carré, B., Taïeb, R., Saliéres, P., 2010. Attosecond imaging of molecular electronic wavepackets. Nat Phys 6, 200 —206.

[22] Torres, R., Siegel, T., Brugnera, L., Procino, I., Underwood, J.G., Altucci, C., Velotta, R., Springate, E., Froud, C., Turcu, I.C.E., Ivanov, M.Y., Smirnova, O., Marangos, J.P., 2010. Extension of high harmonic spectroscopy in molecules by a 1300 nm laser field. Opt. Express 18, 3174 —3180.

[23] Lock, R.M., Zhou, X., Li, W., Murnane, M.M., Kapteyn, H.C., 2009. Measuring the intensity and

phase of high-order harmonic emission from aligned molecules. Chemical Physics 366, 2232.

[24] Smirnova, O., Mairesse, Y., Patchkovskii, S., Dudovich, N., Villeneuve, D., Corkum, P., Ivanov, M.Y., 2009. High harmonic interferometry of multi-electron dynamics in molecules. Nature 460, 972—977.

[25] Za¨ir, A., Siegel, T., Sukiasyan, S., Risoud, F., Brugnera, L., Hutchison, C., Diveki, Z., Auguste, T., Tisch, J.W.G., Saliéres, P., Ivanov, M.Y., Marangos, J.P., 2013. Molecular internal dynamics studied by quantum path interferences in high order harmonic generation. Chemical Physics 414, 184 —191.

[26] Krause, J., Schafer, K., Kulander, K., 1992. High-Order Harmonic-Generation from Atoms and Ions in the High-Intensity Regime. Phys. Rev. Lett. 68, 3535 —3538.

[27] Lewenstein, M., Salières, P., L'Huillier, A., 1995. Phase of the atomic polarization in high-order harmonic generation. Phys. Rev. A 52, 4747 —4754.

[28] Drescher, M., Hentschel, M., Kienberger, R., Uiberacker, M., Yakovlev, V., Scrinzi, A., Westerwalbesloh, T., Kleineberg, U., Heinzmann, U., Krausz, F., 2002. Time-resolved atomic inner-shell spectroscopy. Nature 419, 803 —807.

[29] Chen, M.-C., Hernndez-Garca, C., Mancuso, C., Dollar, F., Galloway, B., Popmintchev, D., Huang, P.-C., Walker, B., Plaja, L., Jaron-Becker, A., Becker, A., Popmintchev, T., Murnane, M.M., Kapteyn, H.C., 2013. Generation of Bright Isolated Attosecond Soft X-Ray Pulses Driven by Multi-Cycle Mid-Infrared Lasers. arXiv:1401.0240 [physics].

[30] Popmintchev, T., Chen, M.-C., Popmintchev, D., Arpin, P., Brown, S., Ališauskas, S., Andriukaitis, G., Balčiunas, T., Mcke, O.D., Pugzlys, A., Baltuka, A., Shim, B., Schrauth, S.E., Gaeta, A., Hernández-García, C., Plaja, L., Becker, A., Jaron-Becker, A., Murnane, M.M., Kapteyn, H.C., 2012. Bright Coherent Ultrahigh Harmonics in the keV X-ray Regime from Mid-Infrared Femtosecond Lasers. Science 336, 1287 —1291.

[31] Tate, J., Auguste, T., Muller, H.G., Salières, P., Agostini, P., DiMauro, L.F., 2007. Scaling of Wave-Packet Dynamics in an Intense Mid infrared Field. Phys. Rev. Lett. 98, 013901.

[32] Pérez-Hernández, J.A., Roso, L., Plaja, L., 2009. Harmonic generation beyond the Strong-Field Approximation: the physics behind the short-wave-infrared scaling laws. Opt. Express 17, 9891 —9903.

[33] Yavuz, I., Altun, Z., Topcu, T., 2012. Wavelength scaling of high-order-harmonic-generation efficiency by few-cycle laser pulses: Influence of carrier-envelope phase. Phys. Rev. A 86, 043836.

[34] Colosimo, P., Doumy, G., Blaga, C.I., Wheeler, J., Hauri, C., Catoire, F., Tate, J., Chirla, R., March, A.M., Paulus, G.G., Muller, H.G., Agostini, P., DiMauro, L.F., 2008. Scaling strong-field interactions towards the classical limit. Nat Phys 4, 386 —389.

[35] Ghimire, S., DiChiara, A.D., Sistrunk, E., Agostini, P., DiMauro, L.F., Reis, D.A., 2010. Observation of high-order harmonic generation in a bulk crystal. Nature Physics 7, 138141.

[36] Gruzdev, V.E., 2007. Photoionization rate in wide band-gap crystals. Phys. Rev. B 75, 205106.

[37] Hawkins, P.G., Ivanov, M.Y., 2013. Role of subcycle transition dynamics in high-order-harmonic generation in periodic structures. Phys. Rev. A 87, 063842.

[38] Oppenheimer, J.R., 1928. Three Notes on the Quantum Theory of Aperiodic Effects. Phys. Rev. 31, 66 —81.

[39] Landau, L. D. and Lifshitz, E. M., Kvantovaya mekhanika (Quantum Mechanics), Fizmatgiz, 1963 (Eng. Transl., Addison-Wesley, Reading, Mass., 1965).

[40] Peremolov, A. M., Popov, V. S. and Terent'ev, M. V., 1966, Ionization of Atoms in an Alternating Electric Field, Sov. Phys. JETP 23, 924 (1966).

[41] Larochelle, S. F. J., Talebpour, A. and Chin, S. L., 1998, Coulomb effect in multiphoton ionization of rare-gas atoms, J. Phys. B 31, 1215 —1224

[42] Nisoli, M., De Silvestri, S., Svelto, O., Szipöcs, R., Ferencz, K., Spielmann, C., Sartania, S., Krausz, F., 1997. Compression of high-energy laser pulses below 5 fs. Opt. Lett. 22, 522 —524.

[43] Guandalini, A., Eckle, P., Anscombe, M., Schlup, P., Biegert, J., Keller, U., 2006. 5.1 fs pulses generated by filamentation and carrier envelope phase stability analysis. J. Phys. B: At. Mol.

Opt. Phys. 39, S257.

[44] Couairon, A., Mysyrowicz, A., 2007. Femtosecond filamentation in transparent media, Physics Reports, 441, 47 —189.

[45] Hauri, C.P., Lopez-Martens, R.B., Blaga, C.I., Schultz, K.D., Cryan, J., Chirla, R., Colosimo, P., Doumy, G., March, A.M., Roedig, C., Sistrunk, E., Tate, J., Wheeler, J., DiMauro, L.F., Power, E.P., 2007. Intense self-compressed, self-phase-stabilized few-cycle pulses at 2um from an optical filament. Opt. Lett. 32, 868 —870.

[46] Berge, L., Skupin, S., Nuter, R., Kasparian, J., Wolf, J.-P., 2007. Ultrashort filaments of light in weakly ionized, optically transparent media. Rep. Prog. Phys. 70, 16331713.

[47] Voronin, A.A., Ališauskas, S., Mücke, O.D., Pugžlys, A., Baltuška, A., Zheltikov, A.M., 2011. High-energy-throughput pulse compression by off-axis group-delay compensation in a laser-induced filament. Phys. Rev. A 84, 023832.

[48] Bergé, L., 2008. Self-compression of 2um laser filaments. Opt. Express 16, 21529 —21543.

[49] Kartashov, D., Ališauskas, S., Pugžlys, A., Voronin, A., Zheltikov, A., Petrarca, M., Béjot, P., Kasparian, J., Wolf, J.-P., Baltuška, A., 2012. White light generation over three octaves by femtosecond filament at 3.9 m in argon. Opt. Lett. 37, 3456 —3458.

[50] Mücke, O.D., Ališauskas, S., Verhoef, A.J., Pugžlys, A., Baltuška, A., Smilgevičius, V., Pocius, J., Giniūnas, L., Danielius, R., Forget, N., 2009. Self-compression of millijoule 1.5 μm pulses. Opt. Lett. 34, 2498 —2500.

[51] Schmidt, B.E., Béjot, P., Giguere, M., Shiner, A.D., Trallero-Herrero, C., Bisson, É., Kasparian, J., Wolf, J.-P., Villeneuve, D.M., Kieffer, J.-C., Corkum, P.B., Légaré, F., 2010. Compression of 1.8 μm laser pulses to sub two optical cycles with bulk material. Appl. Phys. Lett. 96, 121109.

[52] Trisorio, A., Grabielle, S., Divall, M., Forget, N., Hauri, C.P., 2012. Self-referenced spectral interferometry for ultrashort infrared pulse characterization. Opt. Lett. 37, 2892 —2894 .

[53] Driever, S., Bigourd, D., Fedorov, N., Cornet, M., Arnold, M., Burgy, F., Montant, S., Petit, S., Descamps, D., Cormier, E., Constant, E., Zaïr, A., 2013. Tunable 1.6 to 2 μm near infrared few-cycle pulse generation by filamentation Appl. Phys. Lett 102, 191119 —191119 4.

[54] Zaïr, A., Guandalini, A., Schapper, F., Holler, M., Biegert, J., Gallmann, L., Couairon, A., Franco, M., Mysyrowicz, A., Keller, U., 2007. Spatio-temporal characterization of few-cycle pulses obtained by filamentation. Opt. Express 15, 5394 —5404.

[55] Saliéres, P., Carré, B., Déroff, L.L., Grasbon, F., Paulus, G.G., Walther, H., Kopold, R., Becker, W., Milošević, D.B., Sanpera, A., Lewenstein, M., 2001. Feynmans Path-Integral Approach for Intense-Laser-Atom Interactions. Science 292, 902 —905.

[56] Zaï, A , Holler, M , Guandalini, A , Schapper, F , Biegert, J , Gallmann, L , Keller, U , Wyatt, A. S. , Monmayrant, A , Walmsley, I. A. , Cormier, E , Auguste, T , Caumes, JP , Saliéres, P, 2008. Quantum path interferences in high-order harmonic generation. Phys. Rev. Lett 100, 14, 143902

[57] F. Giammanco, A. Pirri, F. Brandi, M. Barkauskas, W. Ubachs, 2005. Measurements of Chirp-Induced Frequency Shift in High-Order. Harmonic Generation in Xenon. 328 Laser Physics, 15, 2,328 —333.

[58] Seideman, T., 1995. Rotational excitation and molecular alignment in intense laser fields. The Journal of Chemical Physics 103, 7887 —7896.